Physica E 118 (2020) 113955

Contents lists available at ScienceDirect

Physica E: Low-dimensional Systems and Nanostructures

journal homepage: http://www.elsevier.com/locate/physe

An effect of Zn content doping on opto-third order nonlinear characteristics of nanostructured CdS thin films fabricated through spray pyrolysis for optoelectronics

Mohd. Shkir [a,b,*], Mohd Anis [c], S. Shafik [d], M. Aslam Manthrammel [a], M.A. Sayeed [a,f], Mohamed S. Hamdy [e], S. AlFaify [a,**]

[a] Advanced Functional Materials & Optoelectronics Laboratory (AFMOL), Department of Physics, Faculty of Science, King Khalid University, P.O Box-9004, Abha, 61413, Saudi Arabia
[b] Research Center for Advanced Materials Science (RCAMS), King Khalid University, P.O. Box 9004, Abha, 61413, Saudi Arabia
[c] Department of Physics and Electronics, Maulana Azad College of Arts, Science and Commerce, Dr. Rafiq Zakaria Campus, Aurangabad, 431001, Maharashtra, India
[d] Thin Film Physics Laboratory, Department of Physics, Electronics and Photonics, Rajarshi Shahu Mahavidyalaya, Latur, 413512, Maharashtra, India
[e] Chemistry Department, College of Science, King Khalid University, PO Box 9004, Abha, 61413, Saudi Arabia
[f] Faculty of Science, Physics Department, Al-Azhar University, Assiut, 71524, Egypt

ARTICLE INFO

Keywords:
Zn:CdS
Thin films
X-ray diffraction
Optical properties
Dielectric properties
Nonlinear optics

ABSTRACT

The facile and cost-effective fabrication of cadmium sulphide (CdS) thin films with diverse contents of Zn was carried out on substrates of glass which maintained at 300 °C temperature. The grown CdS films are observed to belong monophasic hexagonal system at all Zn contents through structural and vibrational inspections. The values of crystallites size were determined in range of 16–31 nm. The Zn existence and its homogeneity were confirmed by EDX and e-mapping. SEM study displayed the modification in surface topography of CdS films by Zn content. Ultra violet-visible-near infrared spectroscopy study revealed that the grown films are of good optical transparency. The indices of refraction values were estimated and shows the variation in range of 1–2.8 owing to Zn. The PL study propose the applications of grown films in green LEDs as the emission peak has been observed at 513 ± 17 nm. Third-order-nonlinear optics (TONLO) constraints were determined through off and on orifice Z-scan data. The order of the values of TONLO index of refraction and susceptibility was noted of 10^{-8} cm^2/W and 10^{-5} esu, orders correspondingly and found to be enhanced with Zn doping in CdS. Enhancement in optical limiting behaviour of CdS was also noticed when doped with Zn.

1. Introduction

Cadmium sulphide (CdS) is a key ingredients from II-VI semiconducting category and possess a number of applications in the field of sensors, nonlinear, electro-optical, solar cell, devices, photocatalyst etc. [1–3]. The available literature on crystal, nanomaterial and nanostructured thin films based on CdS displayed a huge number of usages. CdS based crystals and films are noticed to be very good in photodetection [4–6]. Materials in form of nanostructured thin films from semiconductors are in huge demand in current scenario for various applications point of view like: TFTs, LEDs, gas sensors, heterojunction solar cell, coatings as surface layers, resister to laser damage, electroluminescence, etc. [7]. In recent past numerous reports are available on film fabrication of pure CdS through a number of procedures. It is interesting to inspect doping consequence on physical properties of CdS, as doping plays a vital role in improvement of such properties to be more applicable in future devices. CdS nanomaterials as well as thin films has been fabricated with several dopants from periodic table like: Cu, Sn, Al, Fe, Eu, Li, Co, Ni, B, Ga, Ag, In, Mn, F, Se etc, [8–26] etc. These reports show that the properties of CdS has been significantly improved with doping. Hence, doping is indigenously employed in CdS to tailor its properties for tailor made applications.

For example, Iorgu et al. reports the synthesis of Zn:CdS nanoparticles (NPs) and studied their structural, optical and photoluminescence properties along with morphology [27]. Yang et al. reported the Zn:CdS nanomaterials and investigated for photocatalytic

* Corresponding author. King Khalid University, Abha, Saudi Arabia.
** Corresponding author.
E-mail addresses: shkirphysics@gmail.com, shkirphysics@kku.edu.sa (Mohd. Shkir), saalfaify@kku.edu.sa (S. AlFaify).

https://doi.org/10.1016/j.physe.2020.113955
Received 7 November 2019; Received in revised form 2 January 2020; Accepted 4 January 2020
Available online 11 January 2020

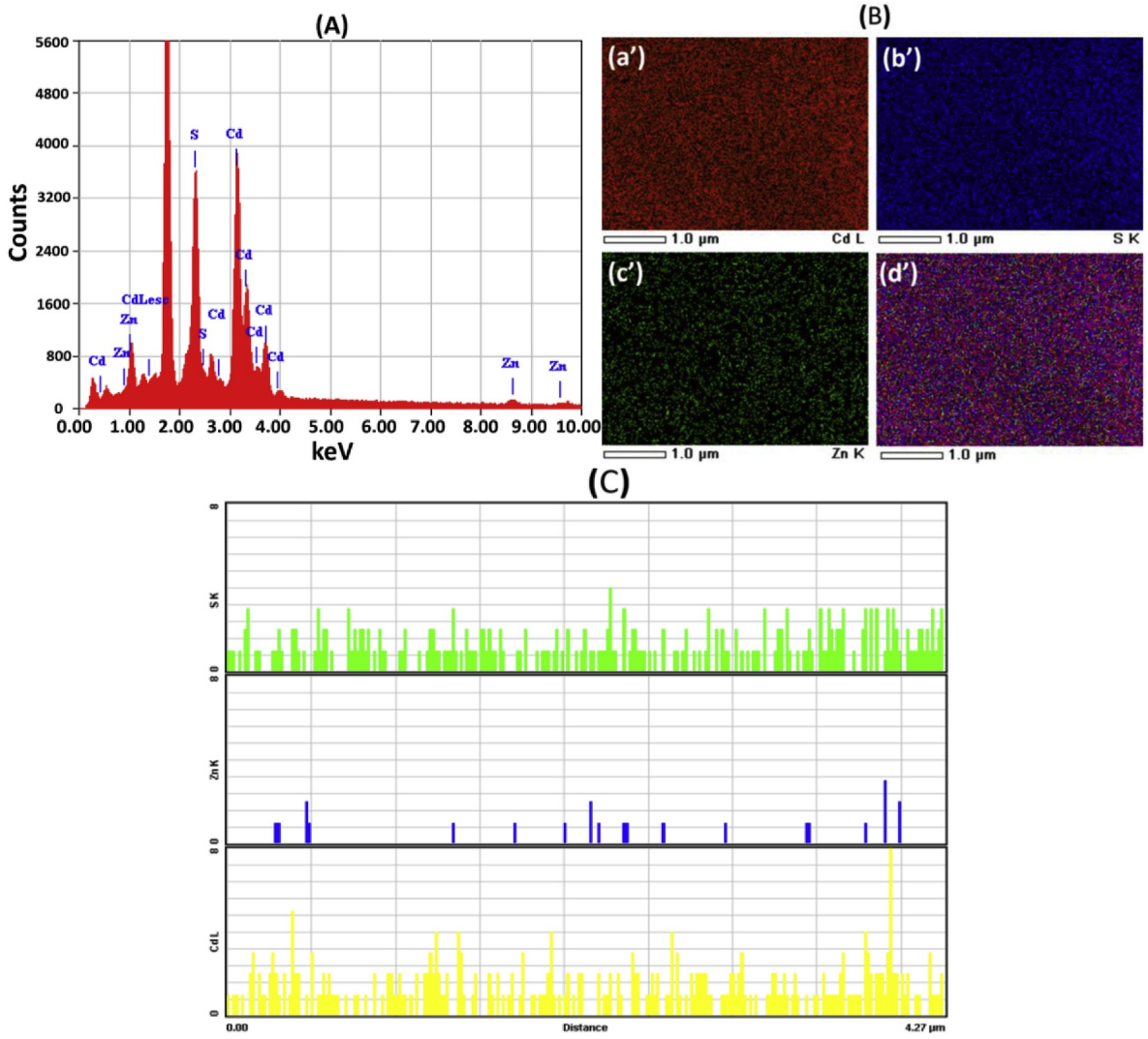

Fig. 1. (A) EDX spectrum, (B) SEM e-mapping and (C) line scan profile of 2.5 wt% Zn:CdS film.

performance under UV [3]. Ibiyemi et al. reported the Zn:CdS NPs synthesis and studied opto-electrical applications [28]. Prabhu et al. prepare a gas sensor based on Zn:CdS/CdTe NPs and studied [29]. Nitsuk et al. prepared the Zn/Co:CdS nanocrystals and investigate structural and optical properties [30]. Very recently a gas sensor based on Zn doped CdS has been fabricated by Huang et al. with astonishing performance [1]. Most of these reports are on Zn:CdS nanostructures.

However, few reports on Zn:CdS films are also available such as: Gu et al. studied the effect of Zn:CdS buffer layer on efficiency of Cu2ZnSnS4 solar cell [31]. Mastia et al. fabricated the films of Zn:Cds by taking 10% solution of Zn precursor through spray pyrolysis and performed the structural, optical and electrical studies [32].

Ma et al. fabricated Zn:CdS films by CBD and performed the structural, optical and electrical investigations [33]. Bakly et al. and Rajathi et al. learnt the fabrication of Cd:ZnS by spin coater for PV applications [34,35]. Anbarasi et al. deposited Zn:CdS films by spray pyrolysis technique and investigated [36]. Liu et al. organised the Zn:Fe:Cds films by MOCVD and studied [37]. Hashim et al. reported the fabrication and analysis of Zn:CdS (Zn at 3, 6 and 9%) films by spray pyrolysis technique [38].

These studies reveal that the doping is a most effective procedure for the improvement of diverse physical characteristics of CdS and Zn^{2+} ion has been chosen here in current to dope in CdS owing to alike structure of ZnS and CdS. The above reports on Zn:CdS signifies that no investigation has been performed on nonlinear performance of CdS with different content doping of Zn deposited by spray pyrolysis technique by Z-scan measurement including several other key parameters in a systematic way. Therefore, the fabrications of 0.0, 0.5, 1.0, 2.5 and 5.0 wt% Zn doped CdS films were achieved through spray pyrolysis route on glass substrate maintained at 300 °C temperature and studies to sightsee the structural-elemental – morphological – optical – photoluminescence – dielectric and nonlinear characteristics and conferred.

2. Investigational procedures

2.1. Fabrication of films and their studies

Hydrated cadmium chloride ($CdCl_2{\cdot}H_2O$), thiourea and Zinc chloride ($ZnCl_2$) were bought from Himedia Pvt. Ltd. Co. of purity 99.9% and applied as it is. For preparing the solutions of Cd and S the required quantity of $CdCl_2{\cdot}H_2O$ and thiourea of 0.025 M in equimolar ratios (1:1) were taken in 5 beakers separately and liquified separately in 18 ml of H_2O:NH_3 (4:1 ratio) under the regular stirring at 300 K by fixing the rotation at 500 rpm. After complete dissolution, both materials were-properly mixed which gives yellow colour solution (of ~36 ml) indicates the formation of CdS in rest of the solutions during the mixing the different content of Zinc chloride (0.5–5.0 wt%) as Zn source were added and proper mixing has been carried out under vigorous stirring at

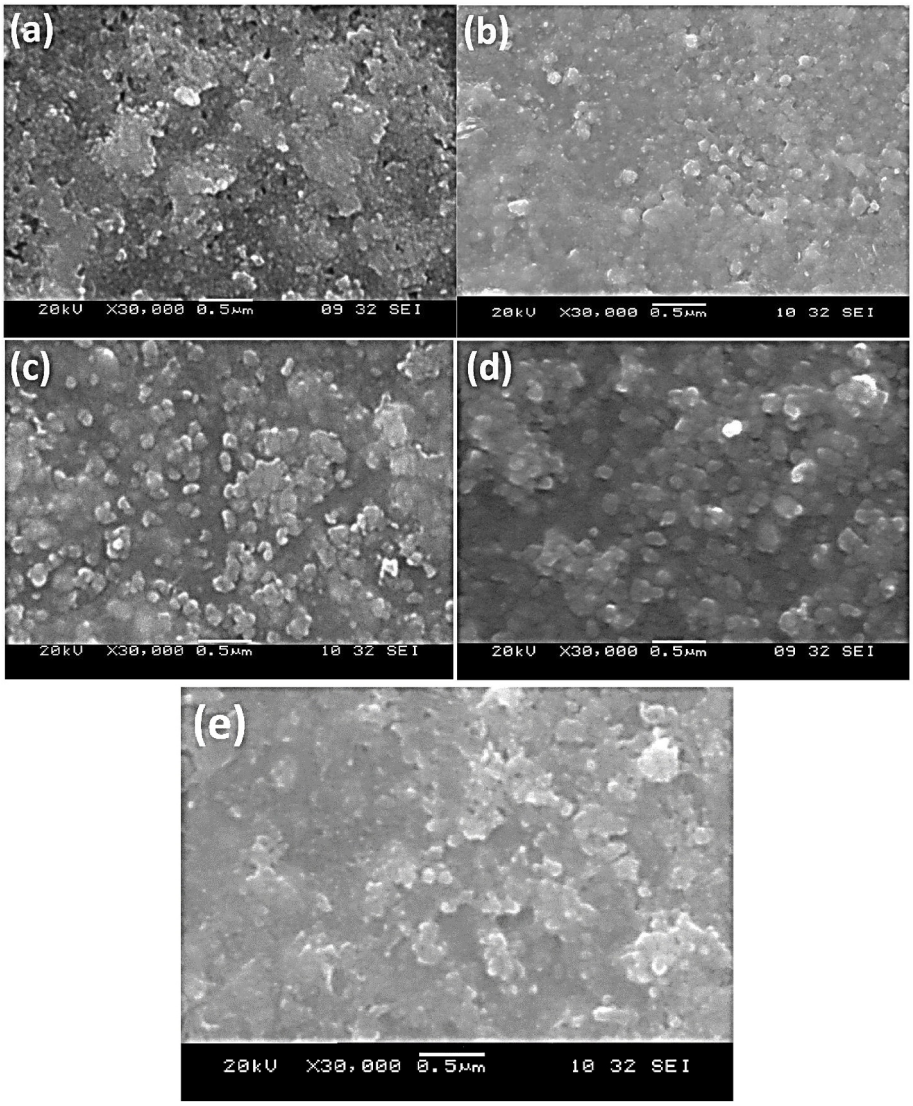

Fig. 2. SEM micrographs for (a) 0.0 wt%, (b) 0.5 wt%, (c) 1.0 wt%, (d) 2.5 wt% and (e) 5.0 wt% Zn:CdS films.

same speed and temperature. All organized solutions were sprayed through spray pyrolizer in which a carrier gas flowing at ~ 1 kg/cm^2 to spray the solution by 5 ml/m on a well-cleaned hot substrate whose temperature was maintained at 300 °C and the distance between spray nozzle and substrate was fixed at 27 cm. After deposition the system was cooled down to room temperature in natural way. The average thickness of grown films was measured through Alpha-Step D-500 Stylus Profilometer and noticed to be 420 nm.

A Lab-X, XRD-6000 (Cu source, $\lambda = 1.54056$ Å) from Shimadzu was used by functioning at 40 kV and 30 mA, over 10–70° angle region at scanning speed of 2°/min for recording the XRD patterns. A 532 nm operated DXR FT-Raman spectrophotometer was used to measure vibrational spectra. JEOL JSM 6360 EDX/SEM system was used to determine elemental and surface tomography. JASCO V-570 UV–Vis.-NIR spectrophotometer for study their linear optical properties. Photoluminescence measurement was performed using Lumina fluorescence spectrophotometer. Third order nonlinear investigations was determined by on and off orifice Z-scan study, using (THORLAB, CW-He-Ne laser, 632.8 nm and 23 mW power).

3. Outcomes and discussion

3.1. Elemental confirmation and morphology studies

For the confirmation of doping element in the films a 2.5 wt% Zn:CdS film was selected to capture the EDX spectra as depicted in Fig. 1(A). However, the presence of Zn was confirmed at other doping content too. Fig. 1(A) reveals the presence of Zn along with Cd and S in the film. The content of Cd, S and Zn was noticed to be 77% (error = 1.1%), 21% (error = 0.72%) and 2.0% (error = 0.25%), correspondingly. To further confirm the distribution of Zn in the films the SEM e-mapping was carried out for each element as represented in Fig. 1B(a'), (b') and (c') for Cd, S and Zn and also their combinational e-mapping was done as depicted in Fig. 1B(d'). These e-mapping indicates the homogeneity of Cd(red), S(blue) and Zn(green) in the final films and Fig. 1B(d') signify the homogeneous distribution of Zn throughout the film. Furthermore, the line scan profile of the film was also recorded as shown in Fig. 1(C), which again confirm the doping level of Zn in CdS films.

SEM images were taken at a fixed magnification, spot size and scale as depicted in Fig. 2(a)–(e). It is noticeable from Fig. 2(a) that the pure films possess some point holes and fine nanoclusters, however when 0.5 wt% Zn is doped in CdS the morphology seems to be totally changed and very few pin holes and absence of cracks has been seen in the films (see

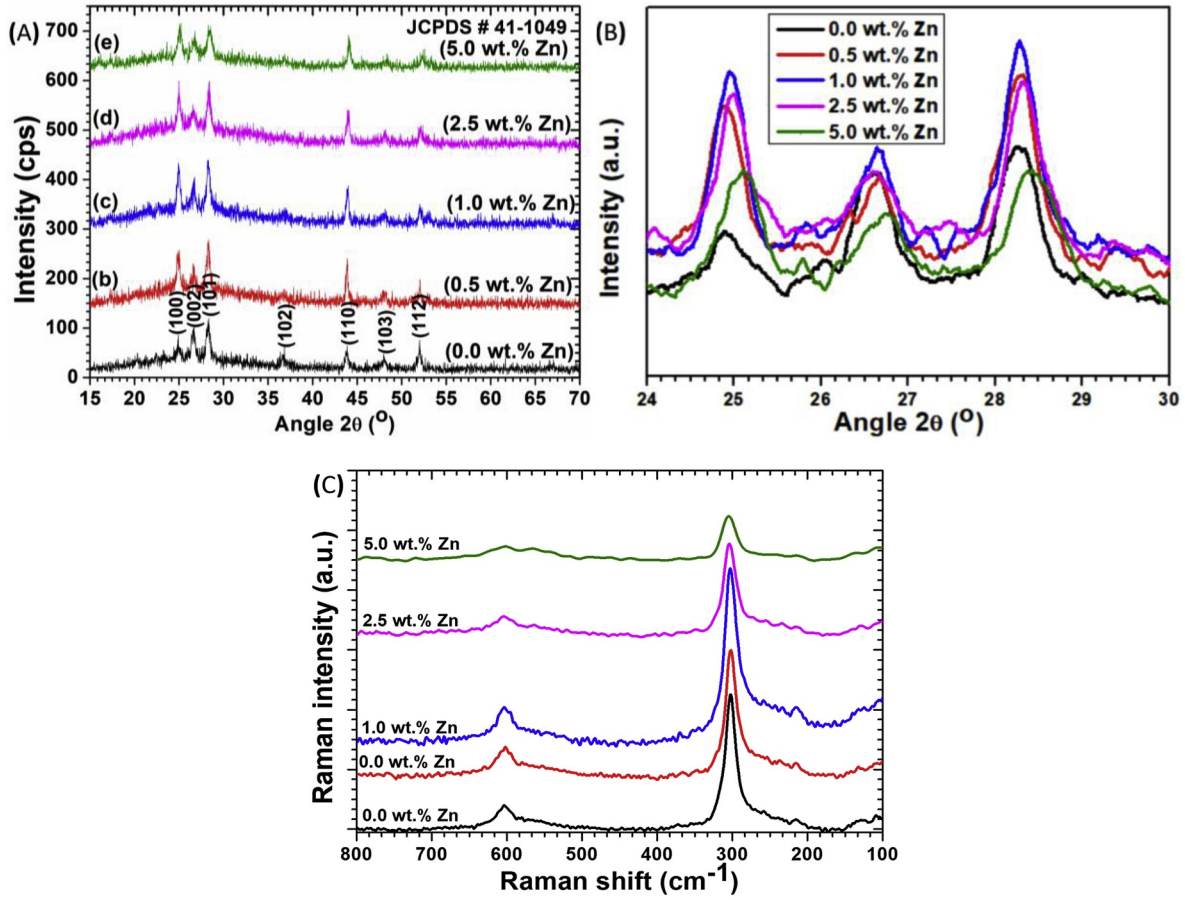

Fig. 3. (A) XRD patterns, (B) Enlarge XRD pattern and (C) FT-Raman spectra for 0.0, 0.5, 1.0, 2.5 and 5.0 wt% Zn:CdS films.

Table 1
Determined values of a, b, c, V, D_{ave}, δ_{ave} and ε_{ave}, and n for Zn:CdS films.

Samples CdS	a = b (Å)	c (Å)	V $(Å)^3$	D_{ave} (nm)	δ_{ave} (lines. nm^{-2}) × 10^{-3}	ε_{ave} × 10^{-3}	n × 10^6
0.0 wt% Zn	4.13897	6.72156	99.72060	30.594	1.299	4.195	15.028
0.5 wt% Zn	4.13940	6.72213	99.74976	19.620	2.741	6.272	3.962
1.0 wt% Zn	4.13999	6.72198	99.77628	20.220	2.494	5.997	4.336
2.5 wt% Zn	4.13957	6.72294	99.76983	20.652	2.499	5.941	4.620
5.0 wt% Zn	4.14171	6.72625	99.92255	16.698	3.881	7.376	2.438

Fig. 2(b)). Also, the grain size has been increased for 0.5 wt% Zn:CdS compare to pure (see Fig. 2(b)) and measured to be ~33 nm (average), however some nanocluster formation was also observed of average size <100 nm. On further increase of Zn content in CdS the films become free from pin holes and cracks however the grain size seems to be rise, up to 2.5 wt% Zn content doping (see Fig. 2(c) and (d)). When the Zn content increased to 5.0 wt% the grain size seems to be reduced compare to 0.5, 1.0 and 2.5 wt% Zn:CdS films and are in nanoclusters form. This indicates that Zn acts a vivacious character in modifying the surface of CdS films and the grain size.

3.2. XRD analysis

The measured XRD patterns with hkl indexing have been displayed in Fig. 3(A). For indexing the peaks position the diffraction pattern was matched with standard JCPDS card no. 41–1049. Also, the lattice constraints were evaluated through POWDERX software and provided in Table 1, which suggest the formation of hexagonal CdS at each Zn content. The lattice constraints are noticed to be varied with Zn content in CdS and well agreed to previous reports JCPDS card No. 89–2944) (a = 4.14 Å, c = 6.715 Å) [1,39].

It is also visible from XRD patterns that no additional phases related to oxides/metal/sulphides like: Zn/Cd/ZnS/ZnO/CdO/ZnO are observed in final products, signify that the doping of Zn content does not affect the hexagonal wurtzite CdS system [33]. Moreover, to have clear indication of XRD peak positions with Zn content the expanded pattern over 24 to 30° has been drawn as depicted in Fig. 3(B). On comparing the XRD pattern in Fig. 3(B) in respect of pure and doped it is noticed that the peaks are shifting towards larger angles that approved that Zn ions doping in CdS lattice as the ionic radii for Zn (i.e. 74 pm) is smaller compared to Cd (i.e. 95 pm) [1]. The peaks height is noticed to be changed with changing the Zn % in CdS (see Fig. 3(A)), initially the intensity has been enhanced up to 2.5 wt% Zn but later it is reduced for 5.0 wt% Zn. Such variation in peaks intensity is might be owing to variation in crystallite size, as the high intensity indicates low FWHM which result in bigger particle size. The respective average values of size of crystallites (D_{ave}), no. of dislocations (δ_{ave}), microstrain (ε_{ave}) and no. of unit cells (n) per unit volume were estimated through the following equations [40–44]: Dave = 0.9λβcosθ, δave = 15 × εa × D and εave = βcotθ4, and $n = \frac{\pi D^3}{6V}$, and offered in Table 1. The authors mean by average is that these values have been estimated for all visible XRD

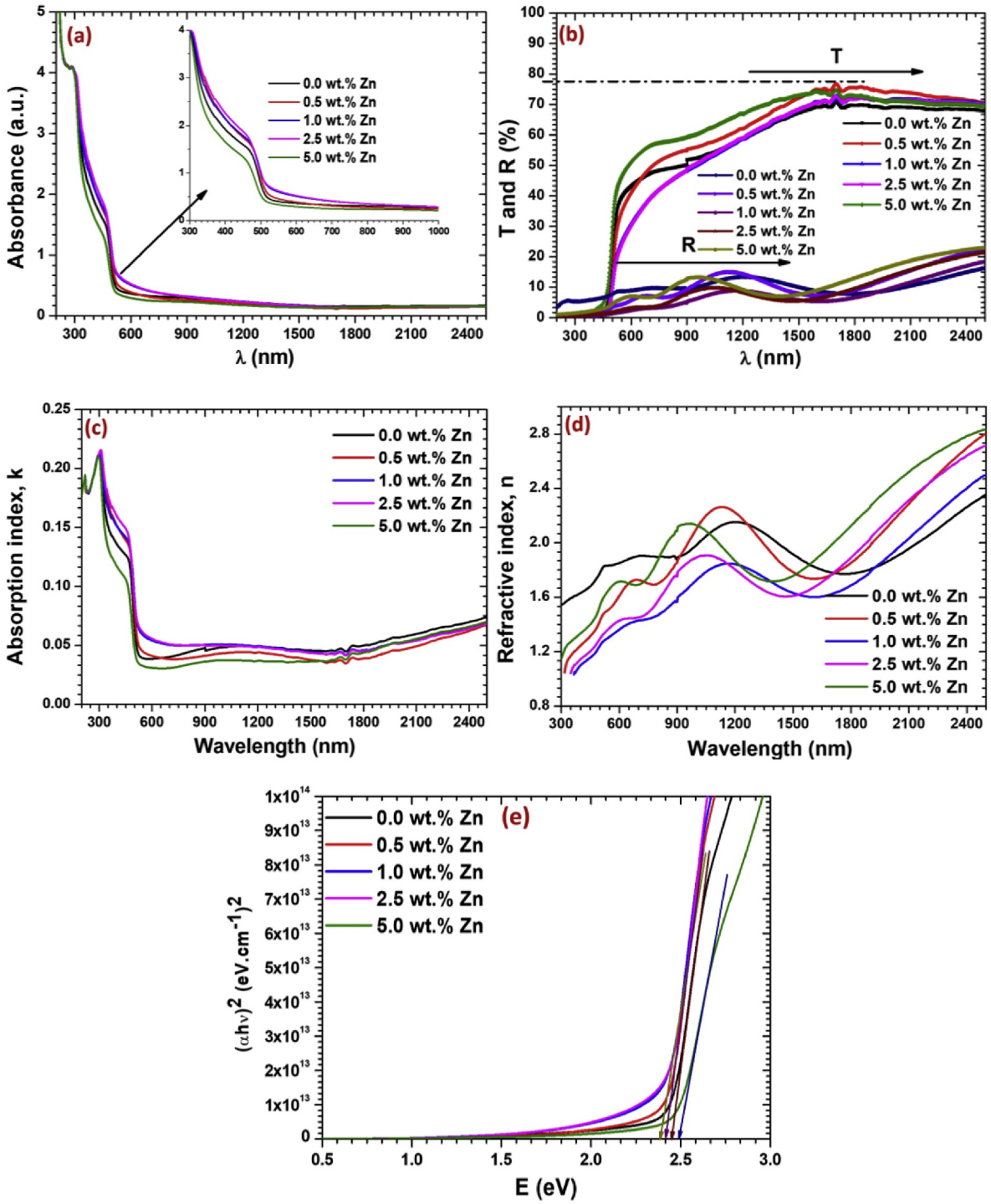

Fig. 4. (a) abs. vs. λ, (b) trans. and refl. vs. λ, (c) absorption index vs. λ, (d) refractive index vs. λ, (e) Tauc's plot for Zn:CdS films.

peaks by taking their FWHM and angular positions. The tabulated values signify that the value of Dave is lessened with Zn content and lowermost value observed for 5.0 wt% Zn:CdS films. In similar fashion of Dave the other values of δ_{ave} and are ε_{ave} also changing with Zn content. Furthermore, the values of number of unit cells in the final products were estimated as given in Table 1, and noted to be reduced with Zn content doping in CdS as it depends on D_{ave} and the value of V [45]. The variation in structural parameters will have clear impact on optical as well as many other properties as studied and discussed in later sections.

3.3. FT-Raman spectroscopy

The measured FT-Raman spectra for Zn:CdS films are depicted in Fig. 3(C), which illustrates that present vibrational modes are well-visible for all films. The intensity of all Raman peaks noticed to varied by varying the Zn. The variation of intensity is also related to full-width at half-maxima of peaks hence changed accordingly. The lowest intensity or broad peaks was distinguished for 5.0 wt% Zn:CdS films which indicates lowest crystallites formation in these films. This was also confirmed by XRD analysis. The FT-Raman comprise two foremost peaks positioned at ~302 ± 3 and 603 ± 3 cm^{-1}, which are assigned for 1LO

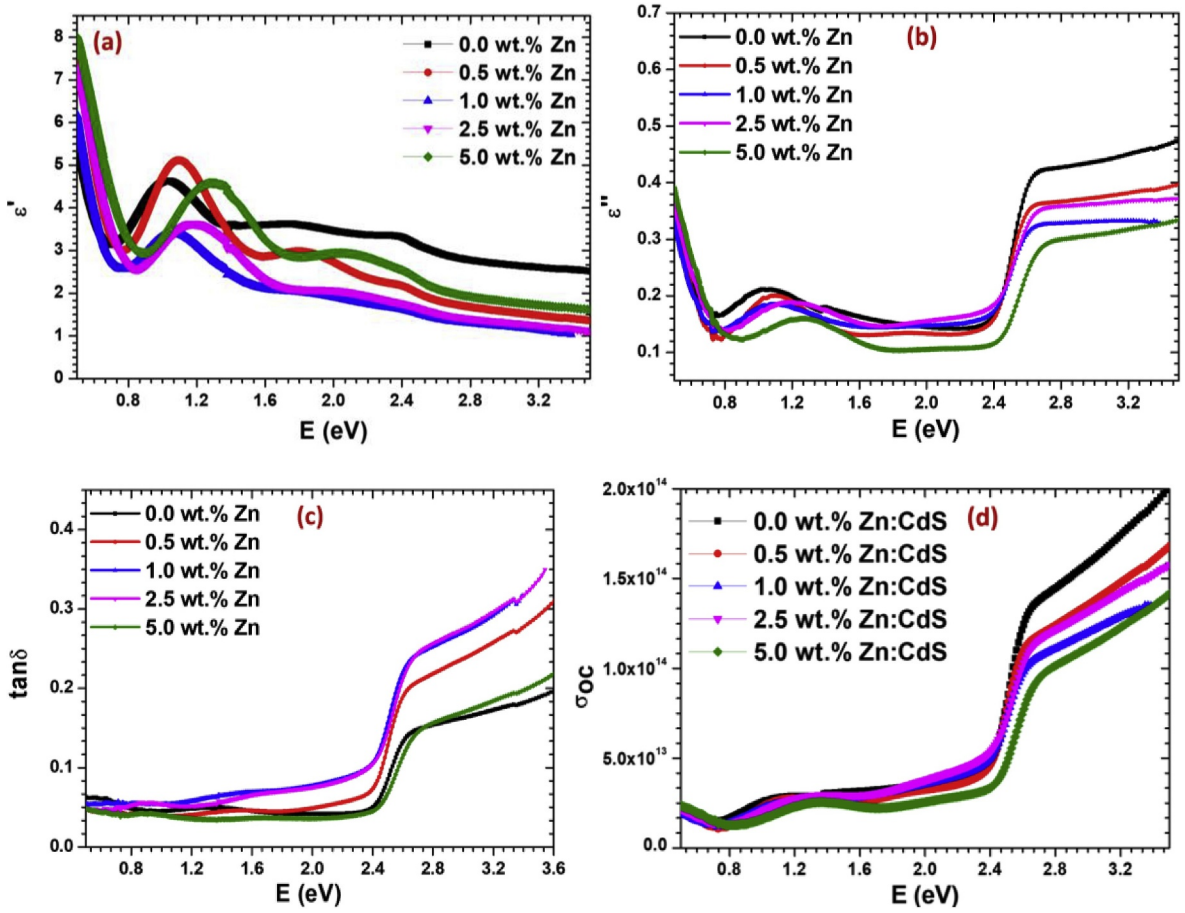

Fig. 5. (a) ε', (b) ε'', (c) loss tangent and (d) optical conductivity for grown Zn:CdS films.

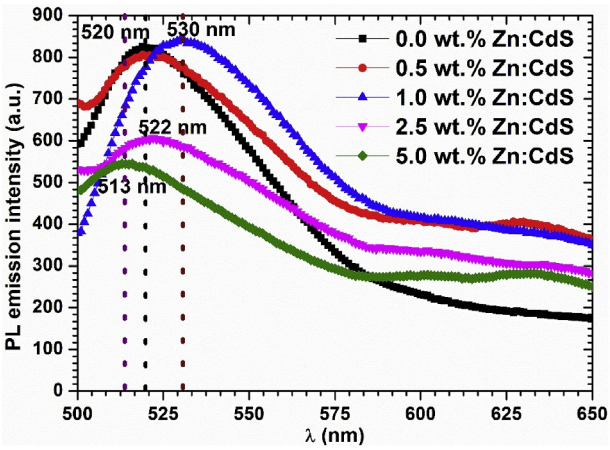

Fig. 6. PL emission spectra for grown 0.0, 0.5, 1.0, 2.5 and 5.0 wt% Zn:CdS films at 450 nm excitation wavelength.

and 2LO phonon modes. These values for CdS crystal are reported at 305 and 611 cm^{-1} [46]. Hence, it is found that the currently observed values are lower compared to bulk one which means nanostructured CdS films formation [47].

3.4. Linear optics and dielectric analyses

To explore the impact of Zn content doping on linear optics of CdS films the UV–Vis_NIR spectra in absorption, transmission and reflection modes was acquired as given in Fig. 4(a) and (b), respectively. Grown films are seeming to own good optical transparency (or possess low absorbance see fig. a) which is in 50–80% range in VIS to NIR region, however stable in NIR region of 1500–2500 nm which is around 70% (see fig. b). Such transparency for coloured material can be considered as good one for optoelectronics. Further, the reflectance is also in accordance to absorbance and transmittance (see Fig. b). It is also visible from figure that the absorption edge is shifting with Zn content in Cds films which results in change of absorption (k) and refractive (n) indices and energy gap (E_g). Such change in absorption edge is might be owing to presence of defects and boundaries in grown films [48]. Hence, the determination of these parameters was carried out through the known process: k = αλ4π, n=(1 + R)(1-R)+4R1-R2-k2 and (αhυ)2 = A(hυ-Eg) (here α = 2.303Absorbanced) (here all other symbols are well-known) [39]. The k & n are graphed in respect of wavelength to Fig. 4(c) and (d), one-to-one. The k and n values are extracted from graphs (c) and (d) and noted in range from 0.03 to 0.22 and 1 to 2.82, correspondingly. These values are noted to be varied throughout the texted region with Zn content doping in CdS films. To note the value of E_g the plot between (αhυ)2 and E(hυ) has been drawn in Fig. 4(e), in which we have sketched a straight line to energy axis at (αhυ)2 = 0 and observed in 2.38–2.50 eV. The obtained E_g values are in agreement to previous reported values [49, 50]. At 0.5, 1.0 and 2.5 wt% the E_g value is decreases from 2.44 to 2.38 eV, however at 5.0 wt% of Zn its value enhanced from 2.44 eV (for pure) to 2.50 eV. The increase in the band gap for the 5.0 wt% Zn sample could be associated to the increase in the film microstrain and decrease in the grain size [15,21]. This indicates a strong effect of Zn on linear optical parameters of CdS films. Such variation in E_g as well as other constraints is might be owing to variation in crystallite size, defect levels/imperfections, compositions, deposition parameters etc. in grown films [51,52].

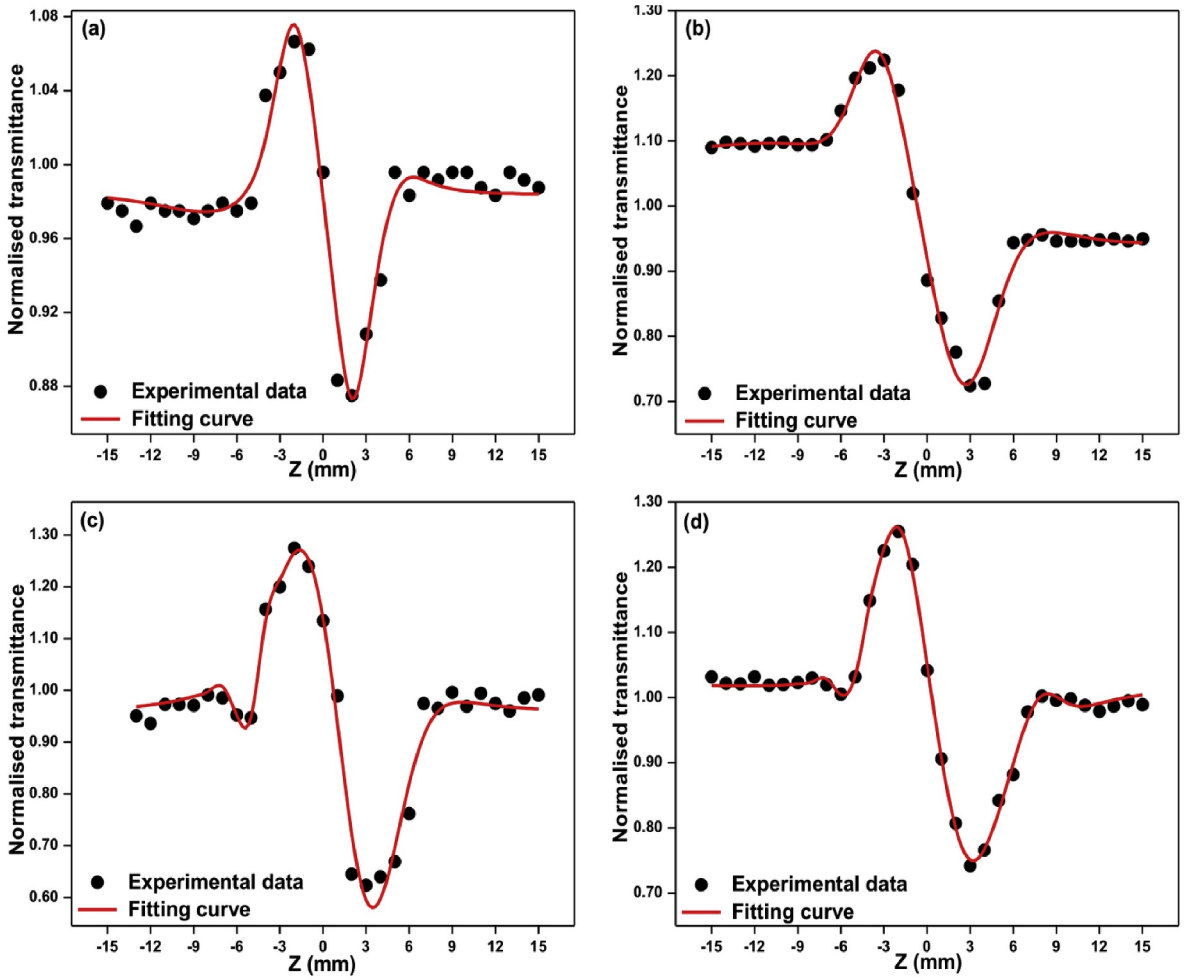

Fig. 7. Close aperture Z-scan curve of (a) 0.5 wt% Zn:CdS (b) 1.0 wt% Zn:CdS (c) 2.5 wt% Zn:CdS (d) 5 wt% Zn:CdS.

The dielectric (real), ε' and loss (imaginary), ε'' values were estimated using the values of n and k above through equations: $\varepsilon' = n2\text{-}k2$, and $\varepsilon'' = 2nk$, $\tan\delta = \varepsilon''/\varepsilon'$ [53] and graphed in Fig. 5(a-c), in respective order. It can be noticed from figures that the values of ε', ε'' and $\tan\delta$ have variation with Zn in CdS and lie in 1–8, 0.1 to 0.5 and 0.02 to 0.35 regions, which are well agreed to previous reports [54]. The low loss values signify the Zn content in CdS reducing the defects in grown films. The optical conductivity was also determined from $\sigma oc = \alpha nc4\pi$ and graphed to Fig. 5(d). The σoc is noted to increase on rising of energy, however reducing with Zn content doping in CdS films and of the order of 10^{14} S/m. It may be mentioned here that the same order should be considered for our previous reported ac conductivity plots [39–42] and also Te:CdS [55].

3.5. Photoluminescence study

The grown films of Zn:CdS were excited at 450 nm to obtain emission spectra (ES) as depicted in Fig. 6 and possess only one major emission peaks. This ES is positioned at 520 nm, 520.5 nm, 530 nm, 522 nm and 513 nm in 0.0, 0.5, 1.0, 2.5 and 5.0 wt% Zn doped CdS. The detected peak of emission is recognised as b-b/Zn created defects emission. The PL emission peak observed in current work is well-agreed to earlier report [56,57]. In all Zn:CdS films only a green emission was noticed which indicates the applications of them in green LEDs. The PL emission peaks is noted to be remarkably shifted by Zn doping in CdS towards higher as well as lower wavelengths. This shift indicates that the enrgy gap of 1.0 wt% Zn:CdS film is lowest one and 5.0 wt% CdS is the largest one which is in accordance with energy gap obtained from Tauc's plot. Moreover, Zn doping also affected the PL intensity which is noted to be quenched with doping except minute increase for 1.0 wt% Zn:CdS film. The intensity variation is related to defects in the grown films.

3.6. Z-scan and optical limiting analysis

Out of the many existing techniques Z-scan is most intriguing way acknowledged by Bahae et al. [58], which can be imposed on range of substrates that are oriented in dimensional order of nano to macro range. Z-scan effectively aids to point out the specific third order nonlinear optical (TONLO) nature, constants and their respective magnitude at a single wavelength which defines its applicability for various photonic device applications as well. The TONLO properties namely nonlinear refraction (n_2) and nonlinear absorption (β) are assessed by off and on orifice of Z-scan arrangement. In present investigation the influence of different concentration of Zn on TONLO constraints of Zn:CdS has been examined by means of CW He-Ne laser functioning at 632.8 nm. The Gaussian filtered beam was focused on each thin film and the transmitted signal was logged by photo-detector located at far distant. The off and on orifice Z-scan transmission curves are represented in Figs. 7 and 8, respectively. The gradual phase alteration near focus ($Z = 0$) point has been revealed owing to irradiation of highly repetitive laser beam confined on the sample leading to divergence of energy along the film plane showing the thermal lensing effect [39,59]. The on orifice Z-scan plot divulges that Zn:CdS film offers the saturable-absorption (SA) effect [60] and SA is usually contributed by domination of ground state over excited state absorption [61]. TONLO susceptibility (χ^3) is the vital parameter which determines the polarizing

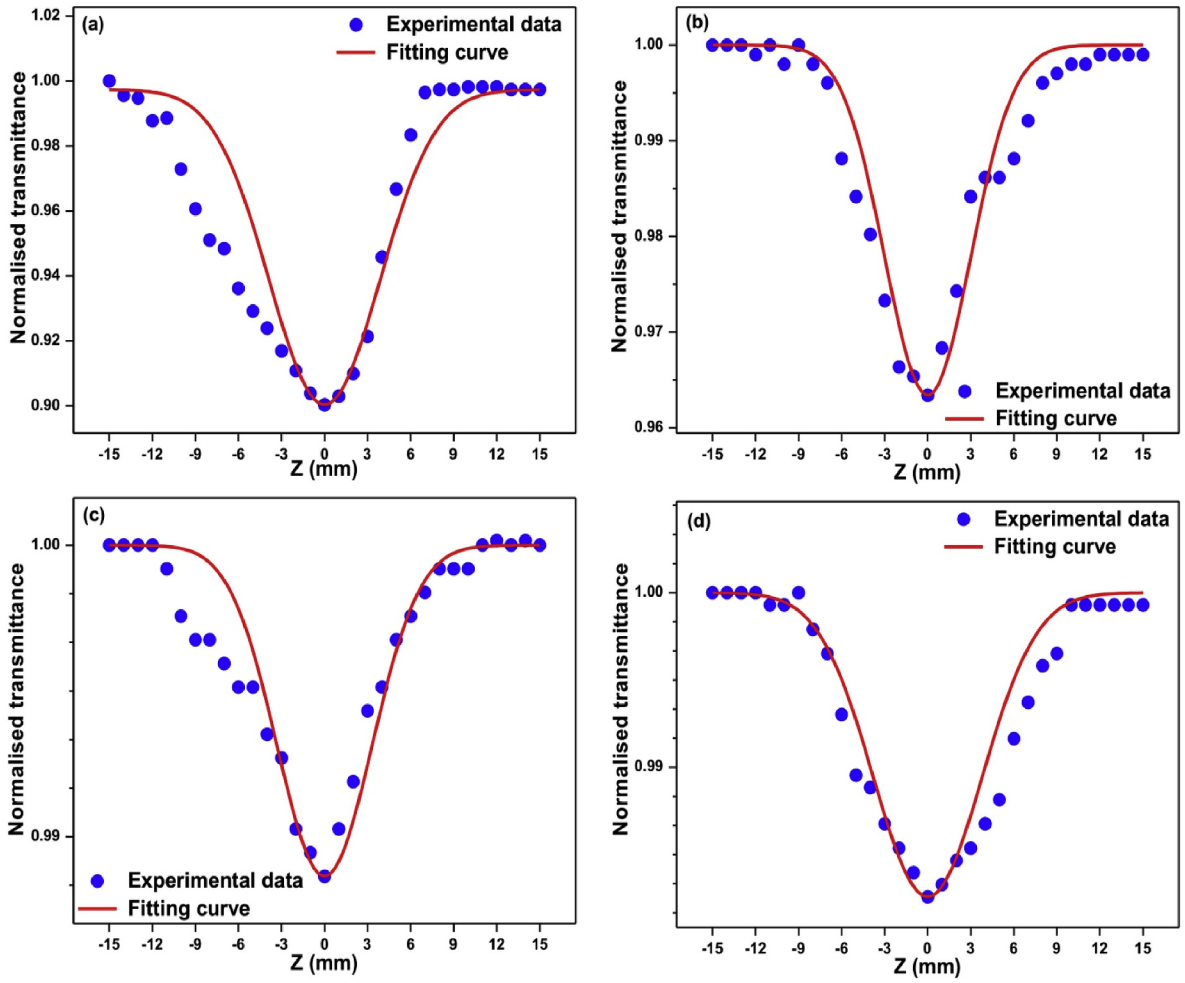

Fig. 8. On orifice Z-scan curve of (a) 0.5 wt% Zn:CdS (b) 1.0 wt% Zn:CdS (c) 2.5 wt% Zn:CdS (d) 5 wt% Zn:CdS.

Table 2
Current and documented comparison of TONLO parameters of Zn:CdS films.

Wavelength	Thin film	n_2 (cm^2/W)	β (cm/W)	χ^3 (esu)	Reference
	0.5 wt% Zn: CdS	2.89×10^{-8}	1.17×10^{-6}	3.68×10^{-5}	Present
632.8 nm	1.0 wt% Zn: CdS	3.44×10^{-8}	2.58×10^{-6}	4.21×10^{-5}	
	2.5 wt% Zn: CdS	3.90×10^{-8}	3.01×10^{-6}	4.99×10^{-5}	
	5.0 wt% Zn: CdS	5.11×10^{-8}	4.66×10^{-6}	6.93×10^{-5}	
	0.5 wt% In: CdS	2.14×10^{-7}	3.12×10^{-3}	4.67×10^{-1}	[39]
	1.0 wt% In: CdS	2.59×10^{-7}	3.99×10^{-3}	5.81×10^{-1}	[39]
632.8 nm	2.5 wt% In: CdS	3.32×10^{-7}	4.75×10^{-3}	6.17×10^{-1}	[39]
	5.0 wt% In: CdS	4.99×10^{-7}	5.37×10^{-3}	7.01×10^{-1}	[39]
	CdS	-1.71×10^{-8}	–	–	[59]
	1 wt% (Nd-Li): CdS-PVP	-2.20×10^{-5}	–	–	[59]
632.8 nm	2 wt% (Nd-Li): CdS-PVP	-2.90×10^{-5}	–	–	[59]
	5 wt% (Nd-Li): CdS-PVP	-3.82×10^{-5}	–	–	[59]
	1 wt% Al:CdS	-5.99×10^{-9}	5.3×10^{-4}	3.64×10^{-5}	[60]
532 nm	5 wt% Al:CdS	-7.48×10^{-9}	6.2×10^{-4}	4.52×10^{-5}	[60]
	10 wt% Al:CdS	-9.84×10^{-9}	7.8×10^{-4}	6.36×10^{-5}	[60]

Table 3
Optical limiting values from Zn:CdS films when tested against red laser of wavelength 650 nm.

The input Intensity (I_o)	Thickness of film	Laser (650 nm) $I_o = 16$ mW	
Samples		Output power, (mW)	Normalized power = output power/input power
0.0 wt% Zn	350	14.20	0.8875
0.5 wt% Zn	350	12.81	0.8006
1.0 wt% Zn	350	10.43	0.6519
2.5 wt% Zn	350	10.10	0.6313
5.0 wt% Zn	350	9.80	0.6125

skill of material [62]. Furthermore, it is noteworthy that the CdS film express positive n_2 which is altered to negative n_2 due to presence of Zn also the nonlinear absorption of CdS film is RSA effect while the Zn:CdS films offers SA as observed in current studies [63]. The TONLO parameters of Zn:CdS films are assessed by formulations derived in documents [58] and these are compared in Table 2. Also the TONLO values are comparable with many previous reported one for diverse materials [64–66]. The current values of nonlinear parameters are also analogous to 2D MXene, Tin Sulfide, Bismuthene, Antimonene, 2D MXene, 2D Graphdiyne and 2D Tellurium documented previously by several authors [67–72]. Tabulated values indicate that the titled grown films are better and equivalent to prior reported one on CdS. The identification of TONLO properties can allow applications in 3D data collection, optical-limiter, faster fluoroscopy, 2P up-conversion lasing, optic pathways, etc [73]. Furthermore, the optical limiting study was carried out using 650 nm red laser of initial intensity ~16 mW. The output values of power intensities are provided in Table 3. Table 3 indicates that the grown films are better as optical limiter when doped with Zn.

4. Conclusion

Zn:CdS thin films were successfully fabricated through spray pyrolysis route on glass substrate. Hexagonal phase of grown films was approved through XRD analysis and this was further supported by FT-Raman study. The D values of grown films lie in range of 16–31 nm. The Zn doping confirmation was approved by EDX and its homogeneity was seen in SEM e-mapping images along with line scan profile. Impact of Zn content on nanostructured morphology of the grown films was confirmed by SEM. The grown films possess better transparency in VIS-NIR region, and the energy gap values are estimated in 2.38 eV–2.50 eV range. The PL study reveals that the grown films possess green emission band with variation in position and intensity with Zn content doping in CdS. The close and open aperture Z-scan data was recorded, and n_2, β and χ^3 values were determined. The values of n_2, β and χ^3 are noticed to be enhanced from Zn doped CdS films from 2.89×10^{-8} to 5.11×10^{-8} cm^2/W, 1.17×10^{-6} to 4.66×10^{-6} cm/W and 3.68×10^{-5} to 6.93×10^{-5} esu in that order. The improvement in optical limiting nature of grown CdS films with Zn doping was also observed. The enhanced values of nonlinear properties propose the grown films favourite for laser devices.

Authors statement

All scientists who meet authorship criteria are listed as authors, and all authors certify that they have participated sufficiently in the work to take public responsibility for the content, including participation in the concept, design, analysis, writing, or revision of the manuscript.

Declaration of competing interest

Authors have no conflict of interest to show.

Acknowledgement

The authors would like to express their gratitude to Deanship of Scientific Research at King Khalid University, Abha, Saudi Arabia for funding this work through Research Groups Program under Grant No. R. G.P. 2/41/40.

References

[1] Z. Huang, D. Wei, T. Wang, W. Jiang, F. Liu, X. Chuai, X. Liang, Y. Gao, P. Sun, X. Yan, J. Zheng, H. Song, G. Lu, Excellent gas sensing of hierarchical urchin-shaped Zn doped cadmium sulfide, J. Alloy. Comp. 773 (2019) 299–304.
[2] J. Jie, W. Zhang, I. Bello, C.-S. Lee, S.-T. Lee, One-dimensional II–VI nanostructures: synthesis, properties and optoelectronic applications, Nano Today 5 (2010) 313–336.
[3] F. Yang, N.-N. Yan, S. Huang, Q. Sun, L.-Z. Zhang, Y. Yu, Zn-doped CdS nanoarchitectures prepared by hydrothermal synthesis: mechanism for enhanced photocatalytic activity and stability under visible light, J. Phys. Chem. C 116 (2012) 9078–9084.
[4] K. Heo, H. Lee, Y. Park, J. Park, H.-J. Lim, D. Yoon, C. Lee, M. Kim, H. Cheong, J. Park, J. Jian, S. Hong, Aligned networks of cadmium sulfide nanowires for highly flexible photodetectors with improved photoconductive responses, J. Mater. Chem. 22 (2012) 2173–2179.
[5] M.A. Mahdi, J.J. Hassan, N.M. Ahmed, S.S. Ng, Z. Hassan, Growth and characterization of CdS single-crystalline micro-rod photodetector, Superlattice Microstruct. 54 (2013) 137–145.
[6] Q. Li, R.M. Penner, Photoconductive cadmium sulfide hemicylindrical shell nanowire ensembles, Nano Lett. 5 (2005) 1720–1725.
[7] A.L. Dawar, J.C. Joshi, Semiconducting transparent thin films: their properties and applications, J. Mater. Sci. 19 (1984) 1–23.
[8] K. Karthik, S. Pushpa, M. Madhukara Naik, M. Vinuth, Influence of Sn and Mn on structural, optical and magnetic properties of spray pyrolysed CdS thin films, Mater. Res. Innov. (2019) 1–5.
[9] A.A. Aboud, A. Mukherjee, N. Revaprasadu, A.N. Mohamed, The effect of Cu-doping on CdS thin films deposited by the spray pyrolysis technique, Journal of Materials Research and Technology (2019).
[10] R. Murugesan, S. Sivakumar, K. Karthik, P. Anandan, M. Haris, Structural, optical and magnetic behaviors of Fe/Mn-doped and co-doped CdS thin films prepared by spray pyrolysis method, Appl. Phys. A 125 (2019) 281.
[11] P. Samiyammal, K. Parasuraman, A.R. Balu, Improved magnetic and photocatalytic properties of spray deposited (Li+Co) codoped CdS thin films, Superlattice Microstruct. 129 (2019) 28–39.
[12] S. Yılmaz, İ. Polat, M. Tomakin, E. Bacaksız, A research on growth and characterization of CdS:Eu thin films, Appl. Phys. A 125 (2019) 67.

[13] I. Yahia, I. El Radaf, A. Salem, G. Sakr, Chemically deposited Ni-doped CdS nanostructured thin films: optical analysis and current-voltage characteristics, J. Alloy. Comp. 776 (2019) 1056–1062.

[14] J. Lee, Raman scattering and photoluminescence analysis of B-doped CdS thin films, Thin Solid Films 451 (2004) 170–174.

[15] H. Khallaf, G. Chai, O. Lupan, L. Chow, S. Park, A. Schulte, Characterization of gallium-doped CdS thin films grown by chemical bath deposition, Appl. Surf. Sci. 255 (2009) 4129–4134.

[16] M. Ristova, M. Ristov, Silver-doped CdS films for PV application, Sol. Energy Mater. Sol. Cells 53 (1998) 95–102.

[17] G. Perna, V. Capozzi, M. Ambrico, V. Augelli, T. Ligonzo, A. Minafra, L. Schiavulli, M. Pallara, Structural and optical characterization of undoped and indium-doped CdS films grown by pulsed laser deposition, Thin Solid Films 453–454 (2004) 187–194.

[18] K. Liu, J. Zhang, X. Wu, B. Li, B. Li, Y. Lu, X. Fan, D. Shen, Fe-doped and (Zn, Fe) co-doped CdS films: could the Zn doping affect the concentration of Fe2+ and the optical properties? Phys. B Condens. Matter 389 (2007) 248–251.

[19] A. Jafari, A. Zakaria, Z. Rizwan, M.S.M. Ghazali, Effect of low concentration Sn doping on optical properties of CdS films grown by CBD technique, Int. J. Mol. Sci. 12 (2011) 6320–6328.

[20] S. Yılmaz, The investigation of spray pyrolysis grown CdS thin films doped with fluorine atoms, Appl. Surf. Sci. 357 (2015) 873–879.

[21] A. Fernández-Pérez, C. Navarrete, P. Valenzuela, W. Gacitúa, E. Mosquera, H. Fernández, Characterization of chemically-deposited aluminum-doped CdS thin films with post-deposition thermal annealing, Thin Solid Films 623 (2017) 127–134.

[22] T. Berus, J. Goc, M. Nowak, M. Oszwałdowski, M. Zimpel, Preparation and electrical properties of InSb thin films heavily doped with tellurium, selenium and sulphur, Thin Solid Films 111 (1984) 351–366.

[23] J. Goral, S.R. Kurtz, J. Olson, A. Kibbler, Transmission electron microscopy study of the effect of selenium doping on the ordering of GaInP 2, J. Electron. Mater. 19 (1990) 95–99.

[24] Y. Gong, Z. Liu, A.R. Lupini, G. Shi, J. Lin, S. Najmaei, Z. Lin, A.L. Elías, A. Berkdemir, G. You, Band gap engineering and layer-by-layer mapping of selenium-doped molybdenum disulfide, Nano Lett. 14 (2013) 442–449.

[25] J. Henry, K. Mohanraj, S. Kannan, S. Barathan, G. Sivakumar, Effect of selenium doping on structural and optical properties of SnS: Se thin films by electron beam evaporation method, Eur. Phys. J. Appl. Phys. 61 (2013) 10301.

[26] A. Kunioka, Y. Sakai, Optical and electrical properties of selenium-cadmium sulfide photovoltaic cells, Solid State Electron. 8 (1965) 961–965.

[27] A. Iorgu, D. Berger, L. Alexandrescu, B. Vasile, C. Matei, Synthesis of photoluminescent pure and doped cadmium sulfide by reverse microemulsion method, Chalcogenide Lett. 10 (2013) 525–531.

[28] A.A. Ibiyemi, A.O. Awodugba, O. Akinrinola, A.A. Faremi, Zinc-doped CdS nanoparticles synthesized by microwave-assisted deposition, J. Semicond. 38 (2017), 093002.

[29] M. Prabhu, V.S. Manikandan, N. Soundararajan, K. Ramachandran, Ethanol gas sensing by Zn-doped CdS/CdTe nanoparticles, AIP Conference Proceedings 1731 (2016), 050141.

[30] Y.A. Nitsuk, M.I. Kiose, Y.F. Vaksman, V.A. Smyntyna, I.R. Yatsunskyi, Optical properties of CdS nanocrystals doped with zinc and copper, Semiconductors 53 (2019) 361–367.

[31] Y. Gu, C. Ye, X. Yin, J. Han, Y. zhou, H. Shen, J. Li, X. Hao, H. Lin, Realizing zinc-doping of CdS buffer layer via partial electrolyte treatment to improve the efficiency of Cu2ZnSnS4 solar cells, Chem. Eng. J. 351 (2018) 791–798.

[32] S. Masti, A. Godghate, A. Patil, M. Jadhav, Study of structural and electrical properties of barium and zinc doped CdS thin film by spray pyrolysis method, Arch. Phys. Res. 5 (2014) 51–55.

[33] L. Ma, X. Ai, X. Wu, Effect of substrate and Zn doping on the structural, optical and electrical properties of CdS thin films prepared by CBD method, J. Alloy. Comp. 691 (2017) 399–406.

[34] A.A.K. Bakly, B.F. Spencer, P. O'Brien, The deposition of thin films of cadmium zinc sulfide Cd1−xZnxS at 250 °C from spin-coated xanthato complexes: a potential route to window layers for photovoltaic cells, J. Mater. Sci. 53 (2018) 4360–4370.

[35] S. Rajathi, R. Vasuki, T.N. Sankarasubramanian, M. Senthamizhselvi, Preparation and characterization of zinc doped CdS thin films for photovoltaic applications, Advances in Natural and Applied Sciences 11 (2017) 144–153.

[36] M. Anbarasi, V. Nagarethinam, A. Balu, Investigations on the structural, morphological, optical and electrical properties of undoped and nanosized Zn-doped CdS thin films prepared by a simplified spray technique, Materials Science-Poland 32 (2014) 652–660.

[37] K. Liu, J.Y. Zhang, X. Wu, B. Li, B. Li, Y. Lu, X. Fan, D. Shen, Fe-doped and (Zn, Fe) co-doped CdS films: could the Zn doping affect the concentration of Fe2+ and the optical properties? Phys. B Condens. Matter 389 (2007) 248–251.

[38] F.S. Hashim, M.A. Habeeb, I.R. Ghanim, Effect of zinc on structural and some optical properties of CdS thin films, Chem. Mater. Res. 3 (2013) 67–74.

[39] M. Shkir, M. Anis, S.S. Shaikh, S. AlFaify, An investigation on structural, morphological, optical and third order nonlinear properties of facilely spray pyrolysis fabricated In:CdS thin films, Superlattice Microstruct. 133 (2019) 106202.

[40] M. Shkir, I.M. Ashraf, S. AlFaify, A.M. El-Toni, M. Ahmed, A. Khan, A noticeable effect of Pr doping on key optoelectrical properties of CdS thin films prepared using spray pyrolysis technique for high-performance photodetector applications, Ceram. Int. (2019).

[41] M. Shkir, I.M. Ashraf, K.V. Chandekar, I.S. Yahia, A. Khan, H. Algarni, S. AlFaify, A significant enhancement in visible-light photodetection properties of chemical spray pyrolysis fabricated CdS thin films by novel Eu doping concentrations, Sens. Actuators A Phys. 301 (2020) 111749.

[42] M. Shkir, Z.R. Khan, M. Anis, S.S. Shaikh, S. AlFaify, A comprehensive study of opto-electrical and nonlinear properties of Cu@CdS thin films for optoelectronics, Chin. J. Phys. 63 (2020) 51–62.

[43] N.J. Suthan Kissinger, M. Jayachandran, K. Perumal, C. Sanjeevi Raja, Structural and optical properties of electron beam evaporated CdSe thin films, Bull. Mater. Sci. 30 (2007) 547–551.

[44] M. Shkir, G. Bhagavannarayana, M. Wahab, K. Maurya, Characterization of ZnTe single crystal grown by Vertical Bridgman Technique using two zone tubular furnace: an important material for optoelectronic devices, Optik-International Journal for Light and Electron Optics 124 (2013) 1995–1999.

[45] M. Shkir, M. Taukeer Khan, V. Ganesh, I.S. Yahia, B. Ul Haq, A. Almohammedi, P. S. Patil, S.R. Maidur, S. AlFaify, Influence of Dy doping on key linear, nonlinear and optical limiting characteristics of SnO2 films for optoelectronic and laser applications, Opt. Laser. Technol. 108 (2018) 609–618.

[46] M. Gilic, J. Trajic, N. Romcevic, M. Romcevic, D. Timotijevic, G. Stanisic, I. Yahia, Optical properties of CdS thin films, Opt. Mater. 35 (2013) 1112–1117.

[47] K. Nanda, S. Sarangi, S. Sahu, S. Deb, S. Behera, Raman spectroscopy of CdS nanocrystalline semiconductors, Phys. B Condens. Matter 262 (1999) 31–39.

[48] A. Kaushal, D. Kaur, Effect of Mg content on structural, electrical and optical properties of Zn1− xMgxO nanocomposite thin films, Sol. Energy Mater. Sol. Cells 93 (2009) 193–198.

[49] A. Cortes, H. Gómez, R.E. Marotti, G. Riveros, E.A. Dalchiele, Grain size dependence of the bandgap in chemical bath deposited CdS thin films, Sol. Energy Mater. Sol. Cells 82 (2004) 21–34.

[50] O. Zelaya-Angel, L. Hernandez, O. de Melo, J.J. Alvarado-Gil, R. Lozada-Morales, C. Falcony, H. Vargas, R. Ramirez-Bon, Band-gap shift in CdS: phase transition from cubic to hexagonal on thermal annealing, Vacuum 46 (1995) 1083–1085.

[51] C. Ramana, R. Smith, O. Hussain, Grain size effects on the optical characteristics of pulsed-laser deposited vanadium oxide thin films, Phys. Status Solidi 199 (2003) R4–R6.

[52] P. Sharma, S.C. Katyal, Effect of deposition parameters on the optical energy gap and refractive index of a-Ge–Se–Te thin films, Philos. Mag. 88 (2008) 2549–2557.

[53] M.-S. Kim, K.-G. Yim, J.-S. Son, J.-Y. Leem, Effects of Al concentration on structural and optical properties of Al-doped ZnO thin films, Bull. Korean Chem. Soc. 33 (2012) 1235–1241.

[54] Z.R. Khan, M. Shkir, V. Ganesh, S. AlFaify, I.S. Yahia, H.Y. Zahran, Linear and nonlinear optics of CBD grown nanocrystalline F doped CdS thin films for optoelectronic applications: an effect of thickness, J. Electron. Mater. 47 (2018) 5386–5395.

[55] S. Mohd, S.S. Shaikh, S. AlFaify, J. Mater. Sci.: Mater. Electron. 30 (2019) 17469–17480.

[56] M.A. Manthrammel, V. Ganesh, S. Mohd, I.S. Yahia, S. Alfaify, Facile synthesis of La-doped CdS nanoparticles by microwave assisted co-precipitation technique for optoelectronic application, Mater. Res. Express 6 (2019), 025022.

[57] A. Khan, M. Shkir, M.A. Manthrammel, V. Ganesh, I.S. Yahia, M. Ahmed, A.M. El-Toni, A. Aldalbahi, H. Ghaithan, S. AlFaify, Effect of Gd doping on structural, optical properties, photoluminescence and electrical characteristics of CdS nanoparticles for optoelectronics, Ceram. Int. 45 (2019) 10133–10141.

[58] M. Sheik-Bahae, A.A. Said, T.-H. Wei, D.J. Hagan, E.W. Van Stryland, Sensitive measurement of optical nonlinearities using a single beam, Quantum Electronics, IEEE J. 26 (1990) 760–769.

[59] S. Azhar, M. Anis, G. Rabbani, M. Shirsat, M. Baig, S. Hussaini, S. AlFaify, M. A. Khan, Growth of NH4H2PO4 crystal in urea environment to optimize linear-nonlinear optical traits for photonic device applications, Optik 185 (2019) 1247–1252.

[60] M. Anis, G. Muley, M. Shkir, S. Alfaify, H. Ghramh, Comparative Analysis on Microhardness and Third Order Nonlinear Optical Traits of Pure and Nd3+ Doped Zinc Tris-Thiourea Sulphate (ZTS) Crystal, Materials Science-Poland, 2018.

[61] G. Ravinder, C. Sreelatha, V. Ganesh, M. Shkir, M.A. Anis, C.R. Rao, Thickness-dependent Structural, Spectral, Linear, Nonlinear and Z-Scan Optical Studies of V 2 O 5 Thin Films Prepared by a Low-Cost Sol-Gel Spin Coating Technique, Materials Research Express, 2019.

[62] S. AlFaify, M. Shkir, V. Ganesh, M. Anis, I. Yahia, A comprehensive investigation on core optoelectronic and laser properties of ZTS single crystals: an effect of Mg 2+ doping, Appl. Phys. B 124 (2018) 196.

[63] S. Talwatkar, A. Sunatkari, Y. Tamgadge, G. Muley, Nonlinear refraction of Nd3+-Li+ co-doped CdS-PVP nanostructure, in: AIP Conference Proceedings, AIP Publishing, 2018, 060004.

[64] N. Priyadarshani, G. Vinitha, T.C. Sabari Girisun, Third order nonlinear optical properties of monoclinic and orthorhombic CuNb2O6 under CW laser illumination, Opt. Laser. Technol. 108 (2018) 287–294.

[65] H. Yao, S. Takahara, H. Mizuma, T. Kozeki, T. Hayashi, Linear and nonlinear optical properties of CdS and CdSe nanoparticles stabilized with poly(N-vinyl-2-pyrrolidone), Jpn. J. Appl. Phys. 35 (1996) 4633–4638.

[66] R. Ganeev, A. Ryasnyansky, S.R. Kamalov, M. Kodirov, T. Usmanov, Nonlinear susceptibilities, absorption coefficients and refractive indices of colloidal metals, J. Phys. D Appl. Phys. 34 (2001) 1602.

[67] L. Wu, X. Jiang, J. Zhao, W. Liang, Z. Li, W. Huang, Z. Lin, Y. Wang, F. Zhang, S. Lu, Y. Xiang, S. Xu, J. Li, H. Zhang, MXene-based nonlinear optical information converter for all-optical modulator and switcher, Laser Photonics Rev. 12 (2018) 1800215.

[68] L. Wu, Z. Xie, L. Lu, J. Zhao, Y. Wang, X. Jiang, Y. Ge, F. Zhang, S. Lu, Z. Guo, Few-layer Tin sulfide: a promising black-phosphorus-analogue 2D material with exceptionally large nonlinear optical response, high stability, and applications in all-optical switching and wavelength conversion, Adv. Opt. Mater. 6 (2018) 1700985.

[69] L. Lu, Z. Liang, L. Wu, Y. Chen, Y. Song, S.C. Dhanabalan, J.S. Ponraj, B. Dong, Y. Xiang, F. Xing, Few-layer bismuthene: sonochemical exfoliation, nonlinear optics and applications for ultrafast photonics with enhanced stability, Laser Photonics Rev. 12 (2018) 1700221.

[70] L. Lu, X. Tang, R. Cao, L. Wu, Z. Li, G. Jing, B. Dong, S. Lu, Y. Li, Y. Xiang, Broadband nonlinear optical response in few-layer Antimonene and Antimonene quantum dots: a promising optical kerr media with enhanced stability, Adv. Opt. Mater. 5 (2017) 1700301.

[71] L. Wu, Y. Dong, J. Zhao, D. Ma, W. Huang, Y. Zhang, Y. Wang, X. Jiang, Y. Xiang, J. Li, Kerr nonlinearity in 2D graphdiyne for passive photonic diodes, Adv. Mater. 31 (2019) 1807981.

[72] L. Wu, W. Huang, Y. Wang, J. Zhao, D. Ma, Y. Xiang, J. Li, J.S. Ponraj, S. C. Dhanabalan, H. Zhang, 2D tellurium based high-performance all-optical nonlinear photonic devices, Adv. Funct. Mater. 29 (2019) 1806346.

[73] R. Bairy, A. Jayarama, G. Shivakumar, S.D. Kulkarni, S.R. Maidur, P.S. Patil, Effect of Aluminium doping on photoluminescence and third-order nonlinear optical properties of nanostructured CdS thin films for photonic device applications, Phys. B Condens. Matter 555 (2019) 145–151.